

Simultaneously determination of bisphenol A and uric acid by zinc/aluminum-layered double hydroxide-2-(2,4-dichlorophenoxy) propionate paste electrode

Nurul Syahida Mat Rais¹, Illyas Md Isa^{1,2*}, Norhayati Hashim^{1,2}, Mohamad Idris Saidin^{1,2}, Siti Nur Akmar Mohd Yazid¹, Mohamad Syahrizal Ahmad¹, Rahadian Zainul³, Suyanta⁴, Siriboon Mukdasai⁵

¹ Department of Chemistry, Faculty of Science and Mathematics, Universiti Pendidikan Sultan Idris, 35900 Tanjong Malim, Perak, Malaysia

² Nanotechnology Research Centre, Faculty of Science and Mathematics, Universiti Pendidikan Sultan Idris, 35900 Tanjong Malim, Perak, Malaysia

³ Department of Chemistry, Faculty of Mathematics and Natural Science, Universitas Negeri Padang, West Sumatera 25171, Indonesia

⁴ Department of Chemistry Education, Faculty of Mathematics and Natural Science, Yogyakarta State University, Indonesia

⁵ Department of Chemistry, Faculty of Science, Khon Kaen University, Khon Kaen 40002, Thailand
*E-mail: illyas@fsmt.upsi.edu.my

Received: 20 March 2019 / Accepted: 8 May 2019 / Published: 30 June 2019

A novel zinc/aluminium-layered double hydroxide-2-(2,4-dichlorophenoxy) propionate (Zn/Al-LDH-DPPA) nanocomposite to modify with multi-walled carbon nanotube (MWCNT) paste electrode for simultaneously determination of uric acid and bisphenol A. The Zn/Al-LDH-DPPA/MWCNT morphology was carried out by a scanning electron microscope and transmission electron microscope, electrode-electrolyte interface properties were examined by electrochemical impedance spectroscopy, and electrochemical responses thoroughly investigated by square-wave voltammetry. The electrode established linear plot for uric acid and bisphenol A from 5.0×10^{-6} M to 7.0×10^{-4} M ($R^2 = 0.9980$) and ($R^2 = 0.9960$) and the detection limits were 7.95×10^{-7} M and 8.71×10^{-7} M (S/N=3). The as-prepared sensor is reproducible, highly stable, sensitive as well as ascribed good anti-interference ability. The Zn/Al-LDH-DPPA/MWCNT electrode is applicable to evaluate simultaneously determination of UA and BPA in lake, river and, urine samples with good percentage recovery.

Keywords: Uric acid; bisphenol A; multi-walled carbon nanotube; square wave voltammetry; zinc layered double hydroxide

1. INTRODUCTION

Bisphenol A (BPA, 2, 2-bis (4-hydroxy phenyl) propane) represented as a typical endocrine disruptor, by mimicking the body's own hormones that will be induced the negative health effects [1,2]. BPA become part of an environmental water monitoring or determining study as their toxicity has attracted vast attention. BPA mainly used to make epoxy resin and polycarbonate plastics. Polycarbonate-based plastics have many applications varying food and drink packaging and medical devices. Unfortunately, under certain condition, BPA has been verified could be concentrated into environment from waste or end-use products such as bottles, packaging, food storage, plastic plants, landfill leachates and thus, could cause danger to public health [3].

Uric acid (UA) is important discovery to track an abnormal level in the human body fluid. UA is the organic heterocyclic compound that found as an end product of purine metabolism, and considered as great importance species in human diagnosis. Extreme abnormalities UA levels may accumulate in urinary system, thus, increase amount in biological fluid had led to severe diseases such as gout or kidney stones [4]; hyperuricemia as a precursor of cardiovascular and renal disease [5] and Lesh-Nyhan syndrome [6]. Otherwise, a decreased UA concentration has been connected to multiple sclerosis, Parkinson's disease, Alzheimer's disease and optic neuritis [7].

Numerous techniques have been previously reported in detecting UA and BPA. Gas chromatography [8], high performance liquid chromatography [9], chemiluminescence [10], enzyme-linked immunosorbent assay [11], fluorescence [12] were widely be used due to efficient detection. However, these techniques is difficult and costly equipment, need to be handled by experienced technicians, slow detection process and complex pre-treatment steps [13]. By comparison, electrochemical sensor is suitable technique that widely used due to cheap equipment, simple procedure, fast reaction, high sensitivity and real-time detection [14].

Layered double hydroxide (LDH) is a composite of anionic clay have been countless reported in research papers due to the use of LDH with various species anions embed into the interlayer region. The intercalation of anionic in LDH open wide significant attention in sensors, catalyst, and adsorbents due to the simple preparation methods by co-precipitation, ion exchange, rehydration using memory effect and hydrothermal method [15]. The contribution of LDH in electrochemical sensor remarkably enhance sensitivity of sensor due to the unique layered structure, ion exchange capabilities and adsorption properties [16].

A few studies reported the capability of several herbicides encapsulated into Zn/Al-LDH interlayer gallery for the determination of various contaminants such as Zn/Al-LDH intercalated 2(3-chlorophenoxy) propionate (Zn/Al-LDH-CPPA) for the determination of cobalt [17], Zn/Al-LDH-3(4-methoxyphenyl)propionate (Zn/Al-LDH-MPP) nanocomposite for the determination of mercury (II) [18], ZLH intercalated 2(3-chlorophenoxy)propionate (ZLH-CPPA) for the determination of copper (II) [19] and ZLH intercalated 3(4-methoxyphenyl) propionate (ZLH-MPP) for the determination of hydrazine [20]. The combination of unique features LDH and anionic herbicides would produce superior properties that would in some way exploited in many applications as well as sensors.

Multi-walled carbon nanotubes (MWCNTs) have captivating countless scientific reports due to electronic properties. To date, their unique properties on having a large surface area and provide high

electrical conductivity are considered promising materials in the fabrication electrode since their application as conducting beneficial in field electron emitting devices would improve performance of sensors [21]. The addition of Zn/Al-LDH nanocomposite into composition MWCNT paste electrode was significantly enhances the resulting current of the electrochemical sensor, thus improving reaction processes. In this study, the potential of Zn/Al-LDH intercalated with 2-(2,4-dichlorophenoxy) propionate herbicides (Zn/Al-LDH-DPPA) in sensor field is greatly investigated.

Beyond of our knowledge, there is no report has been proclaimed about simultaneously detection of UA and BPA using MWCNT modified Zn/Al-LDH-DPPA as modifier in an electrochemical sensor. Hence, the study is proposed to apply the Zn/Al-LDH-DPPA/MWCNT paste electrode towards UA and BPA determinations and the results have presented good sensitivity, low detection limit, wide linear working range, good reproducibility, and stability. The determination of UA and BPA were successfully tested via human urine, lake water, and river water sample with satisfying results.

2. EXPERIMENTAL

2.1. Chemicals and Reagents

Uric acid (UA), bisphenol A (BPA) and potassium chloride were from Sigma-Aldrich (USA), MWCNT from Timesnano (China), paraffin oil (fabrication of paste electrodes), sodium hydroxide, glucose, fructose, sucrose, and both phosphate buffer solution (PBS); K_2HPO_4 and KH_2PO_4 were supplied from Merck (Germany). Supporting electrolyte of 0.1 M PBS was used for entire electrochemical experiments. Stock solutions of 0.01 M UA and BPA were freshly prepared and stored at 4°C. The modifiers, Zn/Al-LDH-DPPA nanocomposite was synthesised according to the previous method [22]. A 4.0 mM potassium ferricyanide (III) $K_3[Fe(CN)_6]$ solution was freshly prepared using 0.1M KCl. Deionized water produced by (Barnstead EASY pure LF, Barnstead, Essex, UK) were used for all solutions.

2.2. Instruments

Square-wave voltammetry (SWV), Cyclic voltammetry (CV), and electrochemical impedance spectroscopy studies (EIS) were conducted using potentiostat model Series-G750 and model Reference 3000 (Gamry, USA). Zn/Al-LDH-DPPA/MWCNT acted as the working electrode, an Ag/AgCl represented as the reference electrode and platinum wire as the auxiliary electrode. The pH measurements were calibrated with standard pH buffer solution firstly, before adjusted with Thermo Scientific Orion 720A Benchtop pH meter (Thermo Fisher Scientific Corp. USA). The morphological studies of Zn/Al-LDH-DPPA and Zn/Al-LDH-DPPA/MWCNT were performed by scanning electron microscope (SEM) and transmission electron microscope (TEM), model SU8020 UHR (Hitachi, Japan).

2.3. Preparation of the MWCNTs/Zn/Al-LDH-DPPA

Fabrication of proposed electrodes were prepared by mixing of total 100 milligram of MWCNT (100.0, 95.0, 90.0, 85.0, 80.0 %, w/w) and with different composition percentage of Zn/Al-LDH-DPPA (0.0, 5.0, 10.0, 15.0 and 20.0 %, w/w) by mixing in a mortar with pestle. Two droplets liquid binder (paraffin oil) was added on top of mixture and mixed until a homogenized paste was obtained. The homogenized paste obtained was firmly packed into Teflon tubes (id = 2.0 mm, 3.0 cm long) and a copper wire was inserted at one end of the tubing to produce electrical contact with the potentiostat.

2.4. Measurement of UA and BPA

Voltammetry measurements were performed on UA and BPA containing 0.1 M PBS (pH 6.0) at the desired concentration. The voltammogram was recorded at range of -0.1 V to $+1.0$ V by utilizing SWV with frequency (180 Hz); pulse height (70 mV); step increment (6 mV). Beforehand to the measurement, the electrode surface was smoothed with filter paper. Every experiment was performed at room temperature of $25 \pm 2^\circ\text{C}$.

2.5. Real Samples

Urine sample of healthy volunteers were collected and 10 ml of urine sample was stored in the refrigerator at $\pm 4^\circ\text{C}$ before filtration. Filter paper used to filter out the residue (diameter $2.5 \mu\text{m}$). Then, the solution was diluted three times (1:3) ratio with PBS. A river water and lake water were used for analysis just after filtration to remove the residue. 10 ml filtered water sample was diluted with PBS, both diluted urine sample and water sample were added a known amount of BPA and UA solution.

3. RESULTS AND DISCUSSION

3.1. Characterization of Zn/Al-LDH-DPPA and Zn/Al-LDH-DPPA/MWCNT

SEM and TEM were utilized to analyze the morphologies of Zn/Al-LDH-DPPA and Zn/Al-LDH-DPPA/MWCNT. Figure 1A show clusters and compact structure in which the existence of the embed anion of DPPA in the gallery of Zn/Al-LDH do not obviously affect the morphology of the materials [23]. The transparent tube of MWCNT clearly be seen in Figure 1B reveal the existence of Zn/Al-LDH-DPPA that was encapsulated by MWCNT [24].

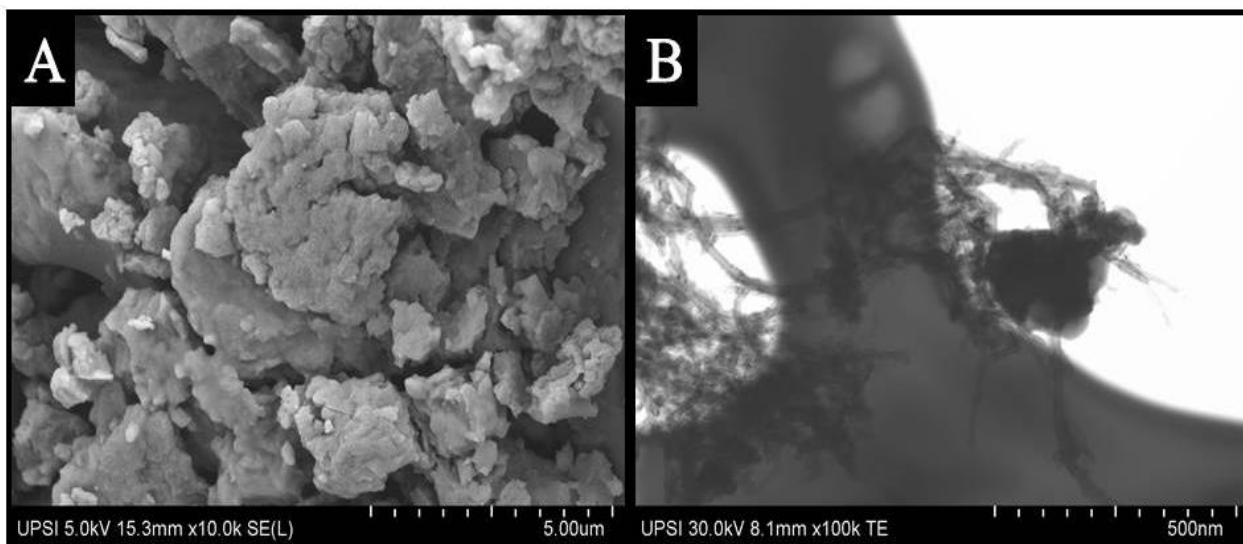


Figure 1. SEM image of (A) Zn/Al-LDH-DPPA and TEM image of (B) Zn/Al-LDH-DPPA/MWCNT.

Ferricyanide, $K_3[Fe(CN)_6]$ is preliminary solution to examine an efficiently of modified electrode by accounting as redox probe in CV firstly. Figure 2A show the cyclic voltammetry for bare MWCNT (curve a) and modified Zn/Al-LDH-DPPA/MWCNT (curve b) in 4.0 mM $K_3[Fe(CN)_6]$. The behaviors of electrodes show that the response were quasi-reversible processes with peak-to-peak separation (ΔE_p) at bare MWCNT, as 371.81 mV and modified Zn/Al-LDH-DPPA/MWCNT, as 395.91 mV. This indicates that relatively the fast electron transfer at modified Zn/Al-LDH-DPPA/MWCNT electrode has improved the current response.

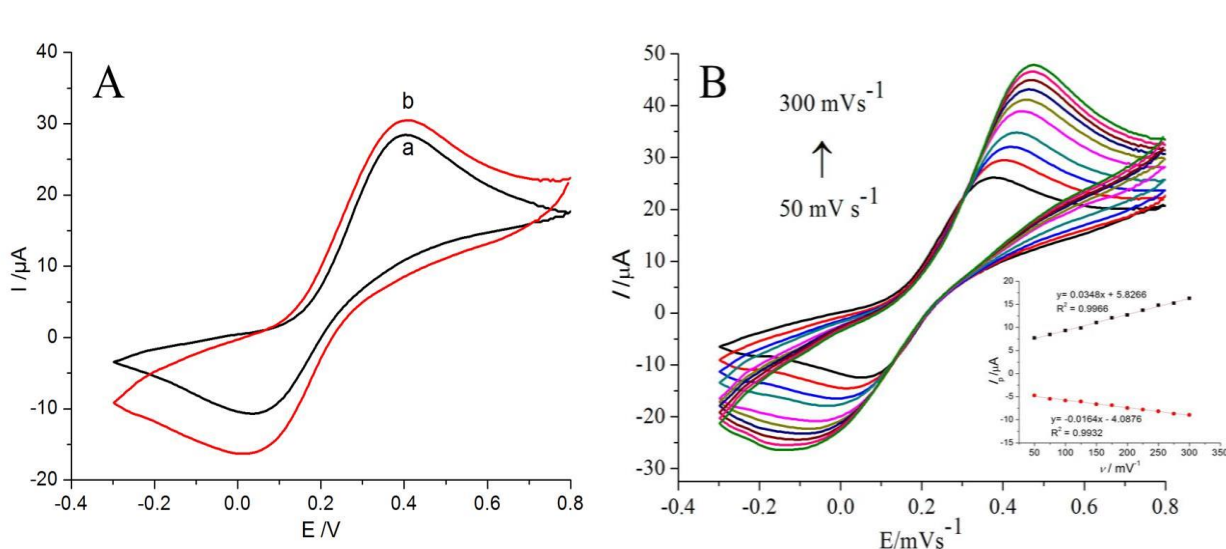


Figure 2. (A) Cyclic voltammety curve of the bare MWCNT (curve a) and modified Zn/Al-LDH-DPPA/MWCNT (curve b) at scan rate of 100 mVs^{-1} and, (B) Cyclic voltammety curve of Zn/Al-LDH-DPPA/MWCNT at various scan rate from 50 to 300 mVs^{-1} , (inset plot : the curve of current vs. square root of scan rate)

Figure 2B presents the cyclic voltammetry of Zn/Al-LDH-DPPA/MWCNT paste electrode in 4.0 mM $K_3[Fe(CN)_6]$. Scanning potential range was used from -0.3V to $+0.8\text{V}$ at scan rates from 50

mV s^{-1} to 300 mV s^{-1} . It was cleared that as the scan rate increase, peak current also will be increased. The regression equations representing anodic peak current $i_{\text{pa}} = 0.915v^{1/2} - 0.05$, with ($R^2 = 0.996$) and cathodic peak current $i_{\text{pc}} = 0.404v^{1/2} - 1.815$, with ($R^2 = 0.993$) demonstrated a good linear relationship with square root of scan rates. This indicated that the Zn/Al-LDH-DPPA modified MWCNT was controlled by diffusion-controlled reaction process [25, 26].

EIS measurement was used to determine the electronic properties of the modified Zn/Al-LDH-DPPA/MWCNT electrode. Figure 3 illustrated the Nyquist plot of (a) bare MWCNT and, (b) modified Zn/Al-LDH-DPPA/MWCNT electrode in $4.0 \text{ mM K}_3[\text{Fe}(\text{CN}_6)]$ solution at frequency range from 1 MHz to 1 Hz . Normally, the Nyquist plots consists of semicircle and a linear portion.

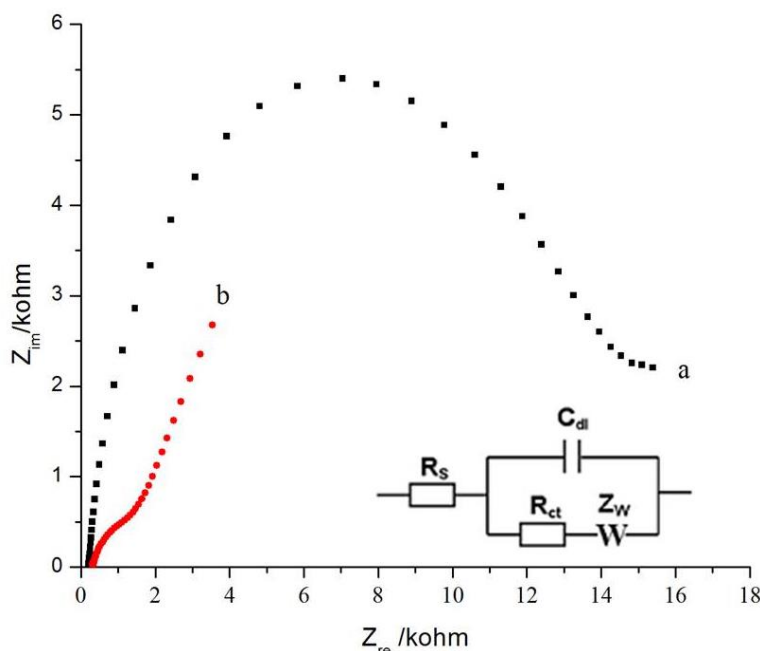


Figure 3. Nyquist plot of (a) bare MWCNT and, (b) modified Zn/Al-LDH-DPPA/MWCNT in a $4.0 \text{ mM K}_3[\text{Fe}(\text{CN}_6)]$ solution.

Electron transfer resistance (R_{ct}) represents by the semicircle diameter acts as kinetic control parameter for interfacial electron transfer at the electrode and linear part represents diffusion process [27]. High R_{ct} ($10.50 \text{ k}\Omega$) was obtained at bare MWCNT and low R_{ct} ($0.5059 \text{ k}\Omega$) at modified Zn/Al-LDH-DPPA/MWCNT indicated that modified the Zn/Al-LDH-DPPA/MWCNT electrode has faster electron transfer process and higher conductivity compared to bare MWCNT. Moreover, the electron-transfer kinetics of both electrodes were determined via electron transfer apparent rate constant, k_{app} in Equation 1 [28];

$$k_{\text{app}} = RT / nF^2 R_{\text{ct}} CA \quad (1)$$

where, R , T , F and C represents the gas constant ($8.314 \text{ J mol}^{-1}\text{K}^{-1}$); absolute temperature (298K); faraday constant (96485 C mol^{-1}); and concentration of $\text{K}_3[\text{Fe}(\text{CN}_6)]$ solution concentration.

The k_{app} value obtained for bare MWCNT was $2.02 \times 10^{-4} \text{ cm s}^{-1}$. After modification of the electrode using Zn/Al-LDH-DPPA/MWCNT, the value of k_{app} raised to $4.19 \times 10^{-3} \text{ cm s}^{-1}$. Large k_{app} value has lower R_{ct} demonstrated that faster electron transfer process between the $K_3[Fe(CN)_6]$ solution and the electrode surface of modified Zn/Al-LDH-DPPA/MWCNT electrode [29, 24].

3.2. Optimization of methods

3.2.1. Effect of pH

The current responses of 0.1 mM UA and BPA was influenced by pH of the analyte solution. In this study, the electrochemical responses towards as-prepared paste electrode were determined in the range of pH 5.0 — 8.0. The result demonstrates that the maximum response peak currents of UA (Figure 4a) and BPA (Figure 4b), both at pH 6.0. A great decreased of the peak current was observed after pH 6.0, indicate that UA and BPA reaction was more actively attracted in acidic medium.

Additionally, Figure 4 also shows the peak potential, E_{pa} for both analytes were shifting to the negative with respect to the increasing of pH values it is conformed to the following equation: $E_{pa} = -0.0597x + 0.78411$ ($R^2 = 0.9971$) and $E_{pa} = -0.0609x + 0.9604$ ($R^2 = 0.9960$). The shift of 59.7 mV/ pH and 60.9 mV/ pH are closely to the Nernst equation slopes theoretical value of 59 mV/ pH, indicated that an equal number (1:1) electron and protons involved in the oxidation of UA and BPA [27, 28]. Thus, pH 6.0 was selected for the up and coming analytical experiments.

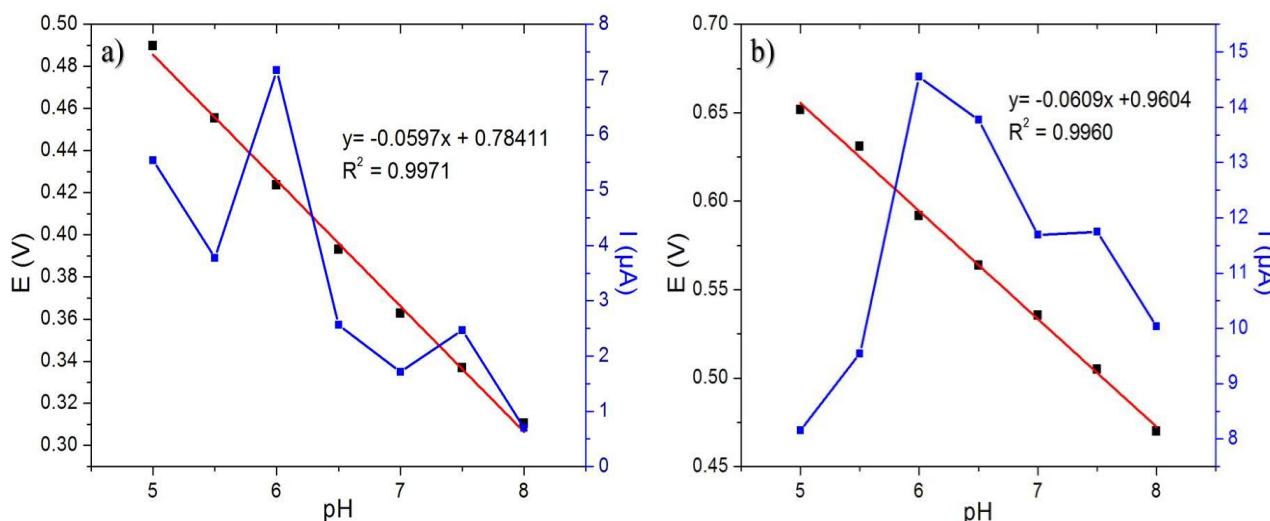


Figure 4. Plot of peak current and peak potential *versus* pH (5.0 to 8.0) of 0.1 mM (a) UA and (b) BPA in 0.1 M PBS ($a = 40 \text{ mV}$, $\Delta E_s = 6 \text{ mV}$, $f = 120 \text{ Hz}$).

3.2.2. Effect of SWV parameters

SWV parameters have been evaluated to identify the best resolution and sensitivity of analytes toward electrodes. The effect of parameters such as frequency, pulse size and step size were further

investigated in 0.1 mM UA and BPA in detail. The effect of frequency was investigated from 30 to 240 Hz at fixed pulse and step size. The peak current shows in Figure 5(a) was gradually increase as increasing of frequency and then reach its optimum frequency at 180 Hz. The effect of pulse size, Figure 5(b) was investigated in the range of 20 to 90 mV. Pulse 80 mV was selected due to highest peak current and generate a good peak resolution. The effect of step size as shown in Figure 5(c) was then studied from 1 to 8 mV at fixed pulse size (80 mV) and frequency (180 Hz). The optimum step size obtained is at 7 mV and was set as highest increments obtained from sensitivity for UA and BPA. Therefore, the optimum SWV parameters that will be used in subsequent studies were frequency =180 Hz, pulse size =80 mV, and step size =7 mV.

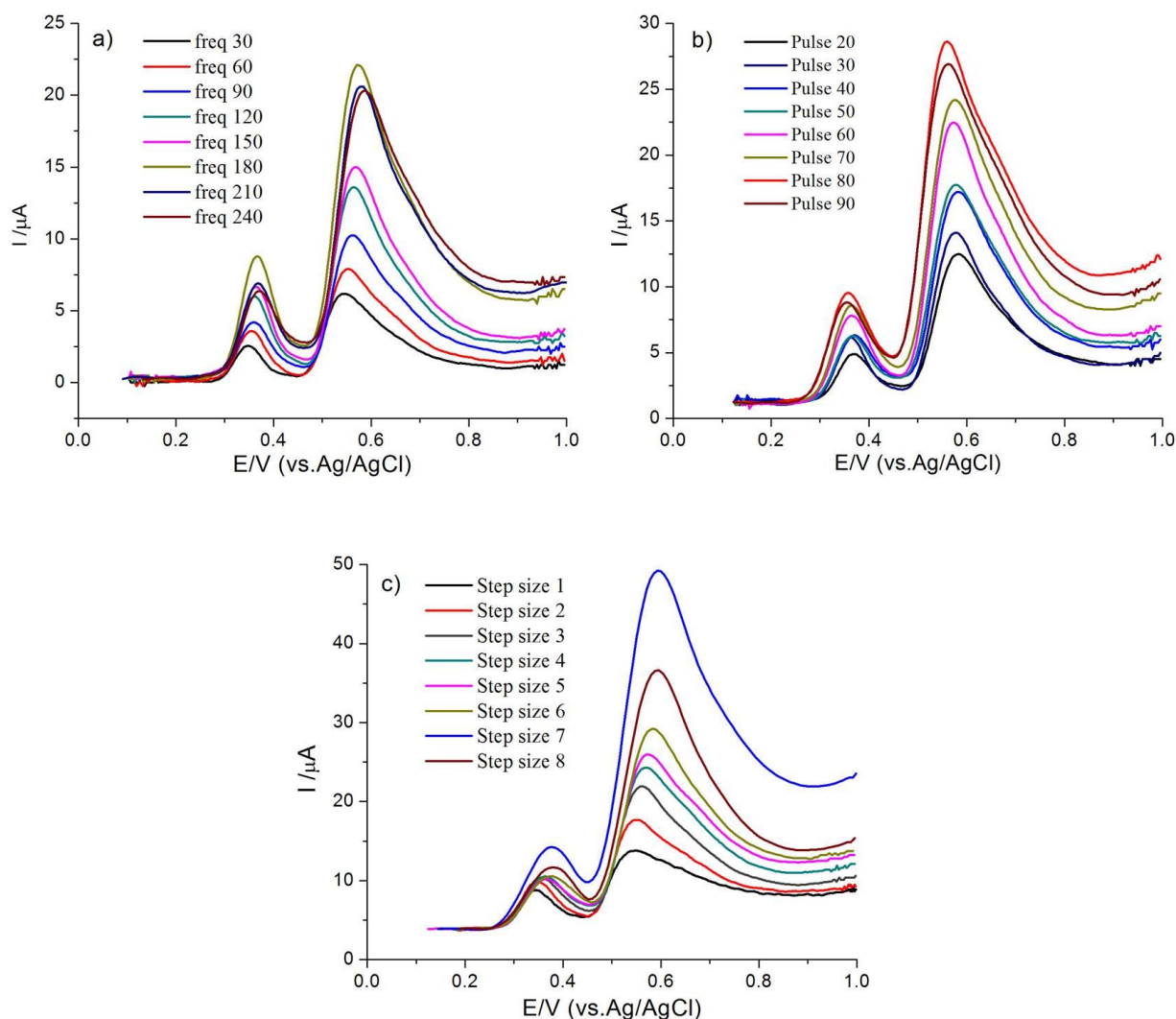


Figure 5. The effect of (a) frequency ($\Delta E_s = 4$ mV, $a = 40$ mV), (b) pulse size ($\Delta E_s = 4$ mV, $f = 180$ Hz), and (c) step size ($a = 80$ mV, $f = 180$ Hz).

3.3. Chronocoulometry

The effective electrochemical surface area (A) of bare MWCNT and modified Zn/Al-LDH-DPPA/MWCNT were investigated by chronocoulometry. The charge (coulombs) produced as a function of time (second) noted as $Q(t)$ was calculated based on Equation (2) given by Anson [32];

$$Q(t) = 2nFAc \left(\frac{Dt}{\pi} \right)^{\frac{1}{2}} + Q_{dl} + Q_{ads} \quad (2)$$

where, $Q(t)$ = Charge (Coulombs); n = Number of electron transfer; F = Faraday constant (96,485 Coulombs/mole); A = Effective electrochemical surface area of the working electrode (cm^2); c = Concentration of substrate (mole/cm^3); D = Standard diffusion coefficient of $\text{K}_3[\text{Fe}(\text{CN})_6]$ is $7.6 \times 10^{-6} \text{cm}^2 \text{s}^{-1}$ at 25°C (as model complex) [33]; t = Time (s); Q_{dl} = Double layer charge (Coulombs); Q_{ads} = Faradaic charge (Coulombs).

$$Q = 76.97 \times 10^{-6} t^{1/2} - 79.14 \times 10^{-6} \quad (3)$$

$$Q = 110.0 \times 10^{-6} t^{1/2} - 60.13 \times 10^{-6} \quad (4)$$

Figure 6A shows the linear regression curves of Q vs $t^{1/2}$ obeys the following equations for bare MWCNT and Zn/Al-LDH-DPPA/MWCNT, respectively. The effective electrochemical surface areas, A was calculated as 0.0641 cm^2 and 0.0917 cm^2 for bare MWCNT and 0.0917 cm^2 for modified Zn/Al-LDH-DPPA/MWCNT. This result revealed the effective electrochemical surface areas were increased greatly after electrodes were modified, which could increase the adsorption capacity of UA and BPA. Thus, improved the current responses and decreased detection limits could be obtained.

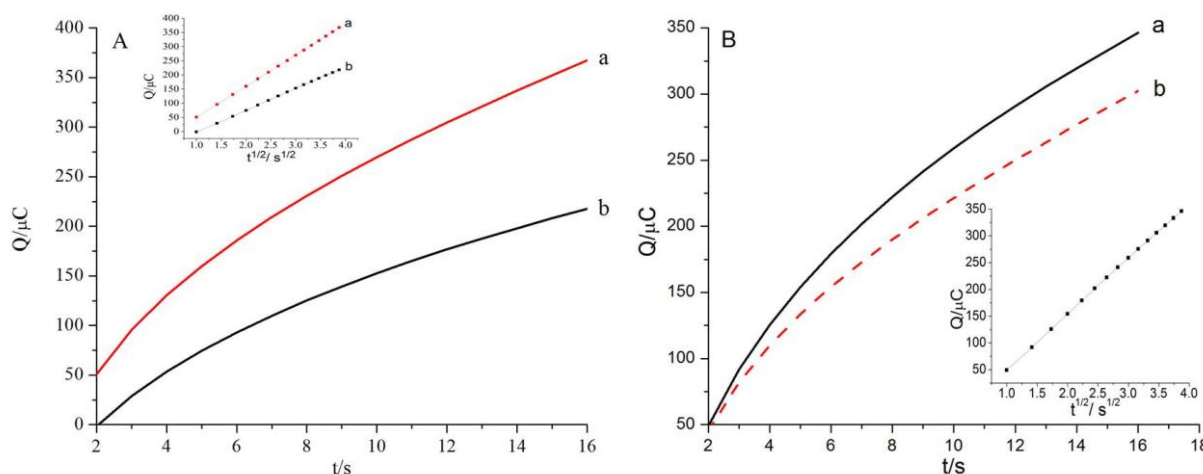


Figure 6. (A) The chronocoulometry plot of (a) Zn/Al-LDH-DPPA/MWCNT paste electrode, and (b) MWCNT paste electrode (B) The chronocoulometry plot of Zn/Al-LDH-DPPA/MWCNT paste electrode (a) in the presence, and (b) absence of 0.1 mM UA and BPA.

The experiments were also performed on modified Zn/Al-LDH-DPPA/MWCNT in the (a) presence and, (b) absence of 0.1 mM BPA and UA, respectively. Figure 6B presents the plot Q against $t^{1/2}$ exhibited linear relationship and was expressed with the following equation:

$$Q = 88.99 \times 10^{-6} t^{1/2} - 44.53 \times 10^{-6} \quad (5)$$

The slope is $8.89 \times 10^{-5} \text{ Cs}^{-1}$ and the intercept (Q_{ads}) is $4.45 \times 10^{-7} \text{ C}$. D calculated to be $1.99 \times 10^{-3} \text{ cm}^2\text{s}^{-1}$ at 25°C , as $n = 2$, $A = 0.0917 \text{ cm}^2$, and $c = 1.0 \times 10^{-4} \text{ M}$. The surface adsorption capacity, Γ_s can be obtained from equation $Q_{\text{ads}} = nFA\Gamma_s$, hence Γ_s calculated was $3.97 \times 10^{-8} \text{ mol cm}^{-2}$, which indicate that modified Zn/Al-LDH-DPPA/MWCNT exhibit a good adsorption capacity for UA and BPA.

3.4. Simultaneously calibration curve

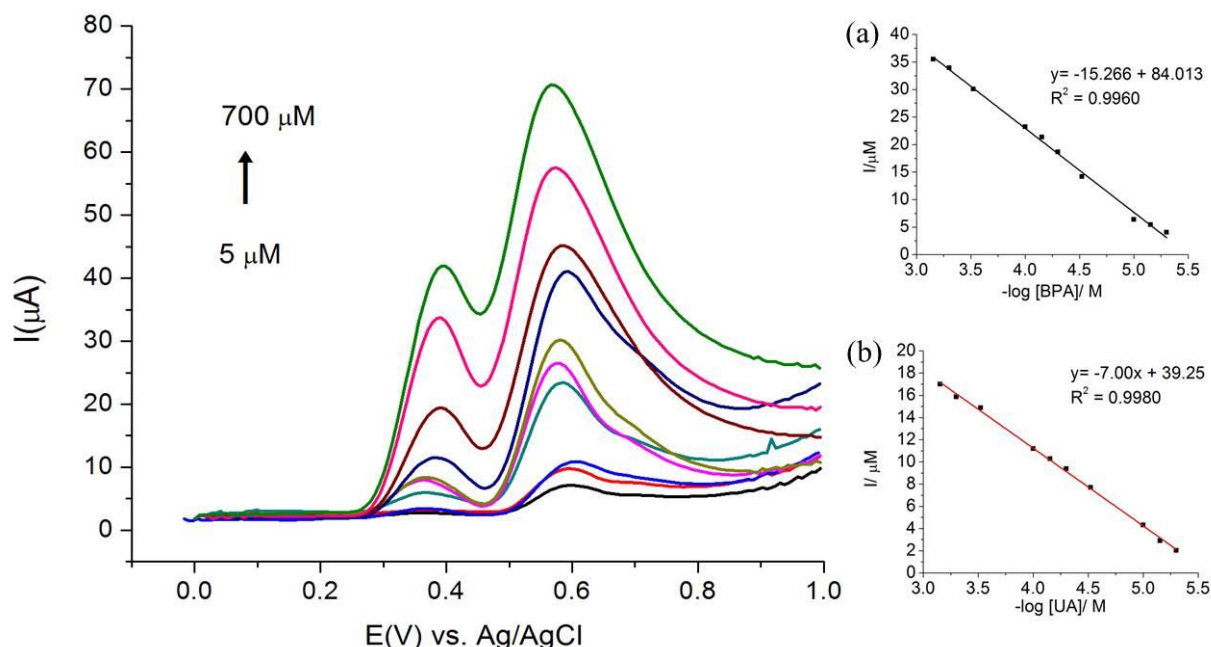


Figure 7. SWV curves of different concentrations of BPA and UA. Inset graph: calibration plot at different concentrations of (a) BPA and (b) UA ($a = 80 \text{ mV}$, $\Delta E_s = 7 \text{ mV}$, $f = 180 \text{ Hz}$).

Table 1. Comparison of Zn/Al-LDH-DPPA/MWCNT paste electrode with others modified electrode for detection of UA and BPA.

Electrode	pH	Working Range (μM)	LOD (μM)	Refs.
Pt-Ni/MWCNT-modified GCE	7	0.1 – 240.4	0.03	[35]
B-MWCNTs	7	62 - 2500	0.65	[21]
$\text{Fe}_3\text{O}_4@/\text{SiO}_2/\text{MWCNTs}$ -CPE	6	0.6 – 100.0	0.13	[36]
AuNCs/AGR/MWCNT/GCE	7	5.0 - 100	0.08	[37]
Pdop@GR/MWCNTs/GCE	7	20 - 320	15	[38]
PGA/MWCNT- NH_2 /GCE	7	0.1 - 10	0.02	[39]
ILs-LDH/GCE	8	0.02 - 3	0.0046	[16]
AuNPs-rGO-MWCNTs/GCE	7	0.005 - 20	0.001	[40]
Ultrathin- $\text{Ni}_2\text{Al-LDH}$ /GCE (ELD)	8.5	0.02 – 1.51	0.0068	[41]
Chitosan/MWCNTs-Au/GCE	8	0.25 - 100	0.083	[42]
Zn/Al-LDH-DPPA/MWCNT/CPE	6	5 - 700	0.795, 0.871	This work

The simultaneously detection of UA and BPA at modified Zn/Al-LDH-DPPA/MWCNT paste electrode was performed by square-wave voltammetry method in their mixture. As UA was increased its concentration in the presence of BPA, it could be observed that both peak currents gradually increased without interfere each other [34]. Figure 7 shows good linearity between peak current vs. UA and BPA concentrations were constructed from 5 μM to 700 μM , respectively. Detection limit ($3\sigma/m$) obtained were 0.795 μM and 0.871 μM for UA and BPA, respectively. Thus, Zn/Al-LDH-DPPA/MWCNT paste electrode was used to simultaneously detect UA and BPA in solution with effective sensitivity. The data collected with the present sensor were compared to other related reported as listed in Table 1.

3.5. Reproducibility, stability and interferences

The reproducibilities of triplicate Zn/Al-LDH-DPPA/MWCNT paste electrodes towards the determination of 0.1 mM UA and BPA were evaluated. The relative standard deviation (RSD) of 3.26% and 4.58% were obtained for UA and BPA, respectively, which revealed that the modified electrode possess good reproducibility. The stability of the electrode was investigated by measure the change of peak current of 0.1mM UA and BPA. The peak current of UA and BPA were slightly decreased to 93.9% and 94.3% from its initial values after 4 weeks suggest the long-term stability and sensitivity of the electrode.

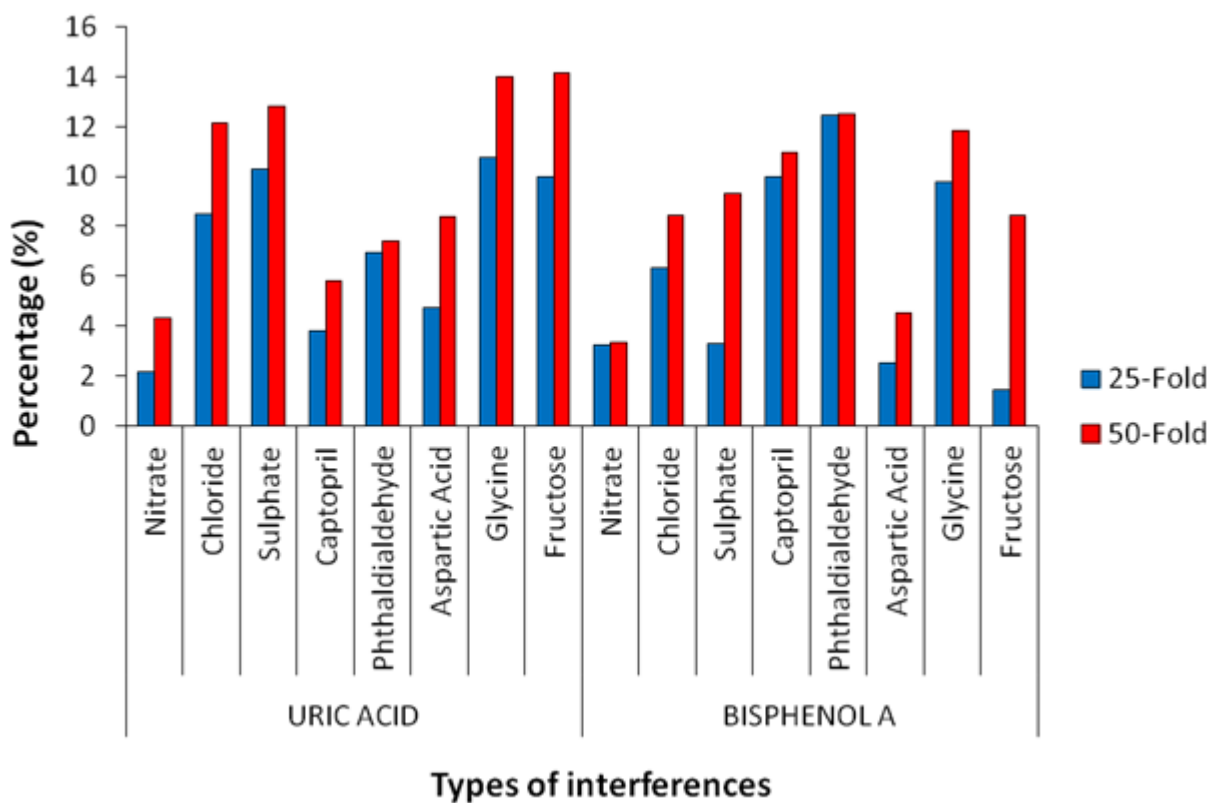


Figure 8. The influence of interfering ions in 0.1 mM UA and BPA at Zn/Al-LDH-DPPA/MWCNT paste electrode ($a = 80 \text{ mV}$, $\Delta E_s = 7 \text{ mV}$, $f = 180 \text{ Hz}$).

The selectivity of the electrode was studied by evaluating the effect of potential interferences at 25-fold and 50-fold excess in the detection of 0.1 mM UA and BPA (Figure 8). Under optimum conditions, the effect of interferences such as NO_3^- , Cl^- , SO_4^{2-} , captopril, phthaldialdehyde, aspartic acid, glycine, and fructose are below than 15% tolerance, which referred that the modified electrode exhibits a good selectivity for the detection of UA and BPA.

3.6. Real sample analysis

The applicability of Zn/Al-LDH-DPPA/MWCNT paste electrode in the determination of UA and BPA in river, lake and, urine samples was evaluated by performing a triplicate measurement. The results of percent recoveries found effective for real samples analysis as tabulated in Table 2.

Table 2. Recoveries of UA and BPA in river water, lake water and human urine (n =3).

Samples	Measured (μM)		Spiked (μM)		Found (μM)		Recoveries (%)	
	UA	BPA	UA	BPA	UA	BPA	UA	BPA
River	n.d	n.d	10	6	10.4	5.95	104.7	99.2
Lake	n.d	0.107	10	6	10.3	6.19	102	101.4
Urine 1	33.7	n.d	30	50	62.8	50.7	98.6	101.5
Urine 2	28.2	n.d	30	50	56.3	51.2	103.3	102.5

n.d: non-detected

4. CONCLUSIONS

The presence research work reported Zn/Al-LDH-DPPA/MWCNT paste electrode sense platform was designed for determination UA and BPA. Electrochemical observation demonstrated that the Zn/Al-LDH-DPPA/MWCNT has high catalytic activity for UA and BPA with an improved peak current compared to unmodified MWCNT paste electrode based on the large effective electrochemical surface area and high adsorption capacity of UA and BPA. The obtained Zn/Al-LDH-DPPA/MWCNT paste electrode had impressive analytical feature such as wide linear working concentration range (5.0×10^{-6} M to 7.0×10^{-4} M), low detection limit of UA and BPA (7.95×10^{-7} M and 8.71×10^{-7} M, S/N=3). The Zn/Al-LDH-DPPA/MWCNT paste electrode shows remarkable recoveries for determination UA and BPA in river, lake and urine samples.

ACKNOWLEDGEMENTS

This work was supported by the Ministry of Education Malaysia and Universiti Pendidikan Sultan Idris, Malaysia (grant numbers : FRGS 2017-0075-101-02).

References

1. J.G. Teeguarden, A.M. Calafat, X. Ye, D.R. Doerge, M.I. Churchwell, R. Gunawan and M.K. Graham, *Toxicol. Sci.*, 123 (2011) 48.
2. K. Christensen and M. Lorber, *Toxics*, 2 (2014) 134.
3. Y. Li, X. Zhai, X. Liu, L. Wang, H. Liu and H. Wang, *Talanta*, 148 (2016) 362.
4. P.E. Erden and E. Kiliç, *Talanta*, 107 (2013) 312.
5. M. Alderman and K.J.V. Aiyer, *Curr. Med. Res. Opin.*, 20 (2006) 369.
6. W.L. Nyhan, *J. Inherit. Metab. Dis.*, 20 (1997) 171.
7. D. Lakshmi, M.J. Whitcombe, F. Davis, P.S. Sharma and B.B. Prasad, *Electroanalysis*, 23 (2011) 305.
8. H.S. Shin, C.H. Park, S.J. Park and H. Pyo, *J.Chromatogr. A.*, 912 (2001) 119.
9. Y. Wen, B. Zhou, Y. Xu, S. Jin and Y. Feng, *J.Chromatogr. A.*, 1133 (2006) 21.
10. C. Lu, J. Li, Y. Yang and J. Lin, *Talanta*, 82 (2010) 1576.
11. E. Maiolini, E. Ferri, L. Pitasi, A. Montoya, M. Di and S. Girotti, *Microchim. Acta*, 139 (2014) 318.
12. L. Du, C. Zhang, L. Wang, G. Liu, Y. Zhang and S. Wang, *Microchim. Acta*, 182 (2014) 539.
13. F. Tan, L. Cong, X. Li, Q. Zhao, H. Zhao, X. Quan and J.Chen, *Sens. Actuators B:Chem.*, 233 (2016) 599.
14. H. Beitollahi and S. Tajik, *Environ. Monit. Assess.*, 187 (2015) 1.
15. D.G. Evans, X. Duan, J. He, M. Wei, B. Li and Y. Kang, *Dev. Clay Sci.*, 119 (2005) 89.
16. T. Zhan, Y. Song, X. Li and W. Hou, *Mater. Sci. Eng. C.*, 64 (2016) 354.
17. I.M. Isa, S.N.A. Dahlan, N. Hashim, M. Ahmad and S.A. Ghani, *Int. J. Electrochem. Sci.*, 7 (2012) 7797.
18. I.M. Isa, S.N.M. Sharif, N. Hashim and S.A. Ghani, *Ionics*, 21 (2015) 2949.
19. N.I. Wardani, I.M. Isa, N. Hashim and S.A. Ghani, *Sens. Actuators B: Chem.*, 198 (2014) 243.
20. I.M. Isa, S. Saruddin, N. Hashim, M. Ahmad and S.A. Ghani, *Int. J. Electrochem. Sci.*, 11 (2016) 4619.
21. N.G. Tsierkezos, U. Ritter, Y.N. Thaha, C. Downing, P. Szroeder and P. Scharff, *Microchim. Acta*, 183 (2016) 35.
22. N. Hashim, M.Z. Hussein, A. Kamari, A. Mohamed, M.S. Rosmi and A.M. Jaafar, *J. Sains dan Mat.*, 4 (2012) 22.
23. M.Z. Hussein, N. Hashim, A.H. Yahaya and Z. Zainal, *J. Exp. Nanosci.*, 5 (2010) 548.
24. M.S. Ahmad, I.M. Isa, N. Hashim, M.S. Rosmi and S. Mustafar, *Int. J. Electrochem. Sci.*, 13 (2018) 373.
25. H. Chen, Z. Zhang, R. Cai, W. Rao and F. Long, *Electrochim. Acta*, 117 (2014) 385.
26. S.N.A.M. Yazid, I.M. Isa, S.A. Bakar and N. Hashim, *Int. J. Electrochem. Sci.*, 10 (2015) 7977.
27. J. Peng, Y. Feng, X.X. Han and Z.N. Gao, *Microchim. Acta*, 183(2016) 2289.
28. E.Sabatani and I.Rubinstein, *J. Phys. Chem.*, 91 (1987) 6663.
29. M.I. Saidin, I.M. Isa, M. Ahmad, N. Hashim and S.Ab Ghani, *Sens. Actuators B:Chem.*, 240 (2017) 848.
30. M.P. Deepak, M.P. Rajeeva and G.P. Mamatha, *Anal. Bioanal. Electrochem.*, 8 (2016) 931.
31. R. Shi, J. Liang, Z. Zhao, A. Liu and Y. Tian, *Talanta*, 169 (2017) 37.
32. F.C. Anson and R.A. Osteryoung, *J. Chem. Educ.*, 60 (1983) 293.
33. J.J. Gooding, V.G. Praig and E.A.H. Hall, *Anal. Chem.*, 70 (1998) 2396.
34. X. Zhang, Y.C. Zhang and L.X Ma, *Sens. Actuators B: Chem.*, 227 (2016) 488.
35. W. Wu, H. Min, H. Wu, Y. Ding and S. Yang, *Anal. Lett.*, 50 (2017) 91.
36. M. Arvand and M. Hassannezhad, *Mater. Sci. Eng. C.*, 36 (2014)160.
37. A.A. Abdelwahab and Y.B. Shim, *Sens. Actuators B: Chem.*, 221 (2015) 659.
38. C. Wang, J. Li, K. Shi, Q. Wang, X. Zhou, Z. Xiong, X. Zou and Y. Wang, *J. Electroanal. Chem.*, 770 (2016) 56.

39. Y. Lin, K. Liu, C. Liu, L. Yin, Q. Kang, L. Li and B. Li, *Electrochim. Acta*, 133 (2014) 492.
40. Y. Hao, F. Xiao, C.X. Xia, G.X. Ling, X. Na and L. Jun, *Chinese J. Anal. Chem.*, 45 (2017) 713.
41. T. Zhan, Y. Song, Z. Tan and W. Hou, *Sens. Actuators B: Chem.*, 238 (2017) 962.
42. W. Guo, A. Zhang, X. Zhang, C. Huang, D. Yang and N. Jia, *Anal. Bioanal. Chem.*, 408 (2016) 7173.

© 2019 The Authors. Published by ESG (www.electrochemsci.org). This article is an open access article distributed under the terms and conditions of the Creative Commons Attribution license (<http://creativecommons.org/licenses/by/4.0/>).